ELSEVIER

Journal of Alloys and Compounds 330–332 (2002) 875–881

Journal of ALLOYS AND COMPOUNDS

www.elsevier.com/locate/jallcom

Highly reflecting Y/Mg–H_x multilayered switchable mirrors

I.A.M.E. Giebels*, J. Isidorsson, E.S. Kooij, A. Remhof, N.J. Koeman, J.H. Rector, A.T.M. van Gogh, R. Griessen

Faculty of Sciences, Division of Physics and Astronomy, Vrije Universiteit, De Boelelaan 1081, 1081 HV Amsterdam, The Netherlands

Abstract

Optical, structural and thermodynamic properties of Y/Mg–H_x multilayered switchable mirrors are investigated and compared with $YMgH_x$-alloys and pure YH_x. Multilayers clearly have superior reflectance in the low-hydrogen state over the whole range of photon energies, $0.72 < \hbar\omega < 3.5$ eV, investigated in this work. In the transparent high-hydrogen state the absorption edge of the multilayers with the *same* overall composition is shifted in energy on increasing the individual layer thicknesses. Thus, the absorption edge is non-trivially depending on the distribution of Mg in the film. Moreover, the optical contrast of multilayers is much higher than for pure YH_x and their optical switching does not suffer from hysteretic effects. Finally, Mg and YH_2 transform almost at the same time to MgH_2 and YH_3, respectively, with a heat of formation of -30.9 kJ/mol H in absorption and -36.6 kJ/mol H in desorption.

PACS: 61.10.Eq; 68.65.+g; 78.40.-q; 78.66.-w; 82.60.Cx; 82.80.Fk

Keywords: ; Hydrogen in metals; YMg hydride; Switchable mirrors; Optical properties; Pressure-composition isotherms

1. Introduction

The optical behaviour of thin, pure yttrium films during hydrogenation is by now well known [1–3]. The shiny metallic films become transparent upon hydrogen uptake. At the same time the material changes from a metal to a semiconductor. At hydrogen concentrations between $1.7 \leq x \leq 2.1$ a weak transmittance window appears in the red part of the visible spectrum ($1.6 \leq \hbar\omega \leq 2.1$ eV). After further hydrogen uptake, the film approaches the composition YH_3 and becomes yellowish transparent (absorption edge at 2.6 eV [4]). Colour neutral switchable mirrors were obtained by Van der Sluis et al. [5] by alloying rare earth (RE) hydrides with magnesium [6–10]. The absorption edge of fully loaded RE–Mg-alloys shifts to higher energies with increasing Mg content [5,10] while the dihydride transparency window of REH_2 is suppressed in the low-hydrogen phase [5]. This, together with the possibility of electrochemical hydrogen loading [2,6,8,11,12], opens the way for technological applications [13]. The suppression of the dihydride transparency window is the result of a 'microscopic shutter effect' which is attributed by Nagengast et al. [9] to the disproportionation of the as-grown YMg intermetallic alloy into YH_3 and insulating MgH_2 during hydrogenation via an intermediate state where metallic Mg coexists with YH_2.

For a better understanding of the role of Mg in switchable mirrors we investigate the optical and thermodynamic properties, the electrical resistivity and the structure of a series of Y/Mg–H_x multilayers with increasing layer thicknesses but the same overall composition of 40 ± 2 at.% Y and 60 ± 2 at.% Mg. The results are compared with a disordered $Y_{0.4}Mg_{0.6}H_x$ alloy and an YH_x-film.

2. Experimental

Polycrystalline Y/Mg multilayers (ML), YMg alloys and Y films with a total thickness of $\approx$150 or 300 nm are deposited at room temperature (for ML) or 100°C (for alloys and Y) in an UHV system (pressure 10^{-9} mbar during evaporation) on quartz and glassy carbon substrates. To prevent the films from oxidation and to catalyze H_2 dissociation a thin palladium cap layer of 10 nm is deposited on top of the film. The following multilayered films are studied: 38*(2 nm Mg + 2 nm Y), 13*(6 nm Mg + 6 nm Y), 15*(10 nm Mg + 10 nm Y), 15*(10 nm Y + 10 nm Mg) + 10 nm Y. These multilayers will be called below 2 nm ML, 6 nm ML and 10 nm ML. Rutherford

*Corresponding author. Tel.: +31-20-444-7925.
E-mail address: giebels@nat.vu.nl (I.A.M.E. Giebels).

0925-8388/02/$ – see front matter
PII: S0925-8388(01)01437-2

backscattering spectrometry (RBS) is used to check the composition. For RBS measurements, films on glassy carbon substrates are used in order to separate the Mg signal from the background signal of the substrate. The samples are contacted ultrasonically with four 30 μm aluminium wires to measure the resistivity with the Van der Pauw method [14].

X-ray diffraction (XRD) measurements are carried out in a RIGAKU X-ray diffractometer, operated in the $\theta-2\theta$ mode using Cu Kα radiation. Dynamic experiments during hydrogen (un)loading are monitored in a relatively limited angular range typically between $26^\circ<2\theta<36^\circ$ with a scan time of approximately 8 min per spectrum. At the same time the resistivity and the transmittance (with a LED, $\lambda_0=635$ nm) of the film are measured. Low-angle reflectivity measurements ($0.2^\circ<2\theta<5.0^\circ$) are performed to study the interface mixing and periodicity of the ML.

Spectrally resolved reflectance and transmittance (R–T) measurements are performed in a Bruker IFS 66/S Fourier transform infrared spectrometer in the energy range $0.72\ \text{eV}<\hbar\omega<3.5$ eV. Reflectance spectra are measured from the backside of the samples through the substrate to circumvent the reflectance of the Pd cap layer.

Finally, electrochemical measurements are carried out using an EG&G Princeton Applied Research 263A Potentiostat/Galvanostat in a three electrode configuration. For single wavelength transmittance measurements a diode laser (Melles Griot, $\lambda=635$ nm (1.96 eV)) is used. More details can be found elsewhere [12].

3. Results and discussion

From low-angle XRD measurements we conclude that the samples are indeed multilayers with the desired periodicity. However, the main multilayer peaks are quite broad. Probably, this is a result of a relatively large layer roughness. In the high-angle XRD spectra of the as-deposited multilayered samples the YMg (110) intermetallic peak can always be distinguished. Since Y and Mg have a large lattice mismatch (~12%), alloying might be a way to release strain in the film [15]. RBS measurements on the 6 and 10 nm ML also show the multilayered structure albeit with a roughness of about 2 nm per layer, which can be attributed to an alloyed interlayer. This interface roughness is consistent with the low-angle XRD measurements.

3.1. Optical properties

To test whether or not the absorption edge of YMg-films is uniquely dependent on the Mg-content we measure the transmittance of the transparent Y/Mg-multilayers and YMg-alloys all with the same overall composition of 40 at.% Y and 60 at.% Mg. Note that MgH_2 is an insulator with an optical gap of approximately 6 eV [16], whereas YH_3 has a gap of 2.6 eV [4].

In Fig. 1 the transmittance spectra of the fully loaded $Y/Mg-H_{2.4}$ multilayers are compared with those of YH_3 and a disordered $Y_{0.4}Mg_{0.6}H_{2.4}$ alloy[1]. The effective optical bandgap, E_g, is estimated from the absorption edges of the spectra using the Lambert–Beer law, $T(\omega)=T_0\exp[-\alpha(\omega)d]$, where α is the absorption coefficient, d the film thickness and T_0 contains the transmittance of the Pd cap layer and the quartz substrate. It can be considered as constant in the region of the absorption edge in our films.

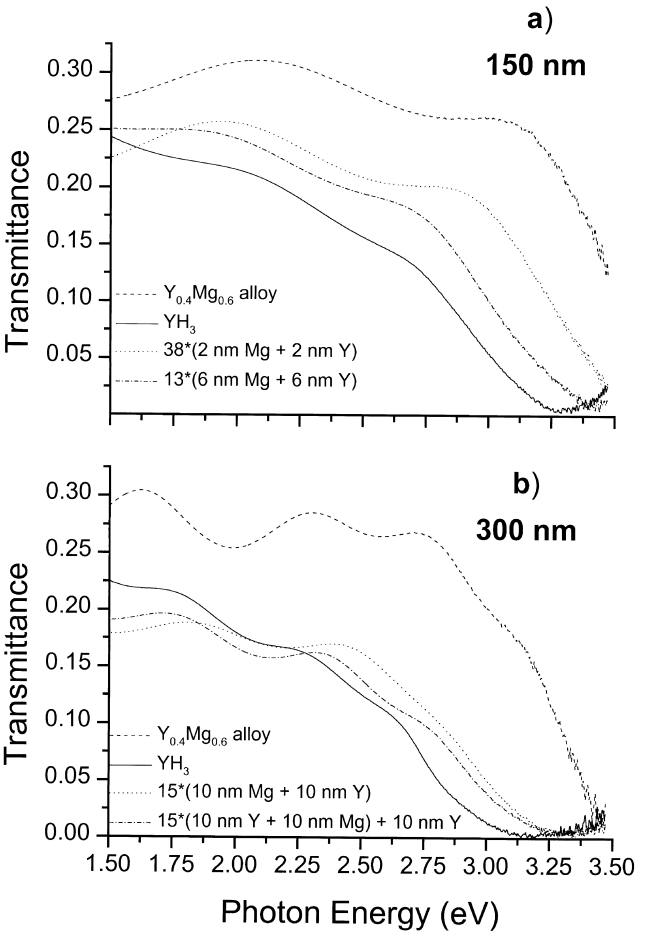

Fig. 1. Transmittance spectra in the fully loaded state of a disordered $Y_{0.4}Mg_{0.6}H_{2.4}$ alloy, $Y/Mg-H_{2.4}$ multilayers of the same overall composition, and YH_3 in the visible part of the optical spectrum (800–350 nm). The films have a total thickness of (a) 150 nm, (b) 300 nm.

[1]The actual hydrogen concentration is not determined in the gas loading experiments. If a sample does not change anymore (optically and electrically) in 1 bar of hydrogen gas, we assume that it is fully loaded and consists of YH_3 and MgH_2. Thus, the hydrogen concentration of the alloy and ML with 40 at.% Y and 60 at.% Mg is 2.4 per atom. After desorption we assume that we have YH_2 and Mg in our films. Thus, the alloys and ML have a hydrogen concentration of 0.8 per metal atom. Note that we did determine the hydrogen concentration in the electrochemical experiment on the 10 nm ML described in Section 3.2. Here you can see that our assumption is in good agreement with the experiment.

The frequency dependence of α near the band edge is related to the (effective) optical gap through [17],

$$\alpha(\omega) \propto \frac{(\hbar\omega - E_g)^{\nu}}{\hbar\omega}, \quad (1)$$

where we take $\nu = 2$ for disordered materials [18]. In Table 1 the resulting effective optical bandgaps are indicated.

In contrast to the observations of Van der Sluis for Gd/Mg–H_x multilayers [19] we observe a clear difference between the fully loaded disordered alloys and the multilayers with the same overall composition (i.e. the same amount of MgH_2 and YH_3). With increasing layer thickness the absorption edge of the multilayers shifts in energy from that observed in $Y_{0.4}Mg_{0.6}H_{2.4}$ alloys to the edge of pure YH_3. This is accompanied by a shift from colour neutral to yellowish transparent. The transmittance is also decreased with respect to the alloy. Clearly, the transmittance and the absorption edge are non-trivially dependent on the distribution of Mg and Y in the film.

This is possibly due to an irregular distribution of MgH_2 clusters (with a large bandgap [16]) through the alloyed films and ML with very thin layers. However, as discussed by Van der Molen et al. [10] for $Y_{1-x}Mg_xH_y$ alloys, it is more likely that the band structure of YH_3 is changed. This might be a result of quantum confinement effects in the small YH_3 clusters.

In Fig. 2 the reflectance spectra of the Y/Mg–$H_{0.8}$ multilayers are compared with those of YH_2 and the $Y_{0.4}Mg_{0.6}H_{0.8}$ alloy after desorption of hydrogen in air at 100°C[1]. YH_2 exhibits a large dip in the reflectance around 1.75 eV and is even slightly transparent between $1.6 \leq \hbar\omega \leq 2.1$ eV. This weak dihydride transmittance window arises from low free electron absorption around the screened plasma energy, and low interband absorption [4,20]. However, the $Y_{0.4}Mg_{0.6}H_{0.8}$ alloy [5,9] and multilayers do not exhibit such a transmittance window in the low-hydrogen state due to the Mg which acts as a 'microscopic shutter' [9].

The alloy has a rather flat, structureless reflectance spectrum while the 2 nm ML exhibits a large enhancement of the reflectance over the whole energy range. This is probably related to the presence of highly reflecting metallic Mg layers in the multilayer, whereas in the alloy only small Mg grains exist. The 6 and 10 nm multilayers exhibit an intermediate behaviour in between the alloy and the 2 nm ML. If we now put Y as a first layer on the substrate instead of Mg, the YH_2 character becomes more pronounced and the reflectance drops below that of the alloy (see Fig. 2b).

Table 1
Effective optical bandgap of YH_3, $Y_{0.4}Mg_{0.6}H_{2.4}$ alloy and Y/Mg–$H_{2.4}$ multilayers obtained from a fit to the absorption edges of Fig. 1 using the Lambert–Beer law and Eq. (1) with $\nu = 2$

Sample	E_g (±0.1 eV)
$Y_{0.4}Mg_{0.6}H_{2.4}$ alloy	3.1
38*(2 nm Mg + 2 nm Y)	2.9
13*(6 nm Mg + 6 nm Y)	2.7
15*(10 nm Mg + 10 nm Y)	2.7
15*(10 nm Y + 10 nm Mg) + 10 nm Y	2.7
YH_3	2.6

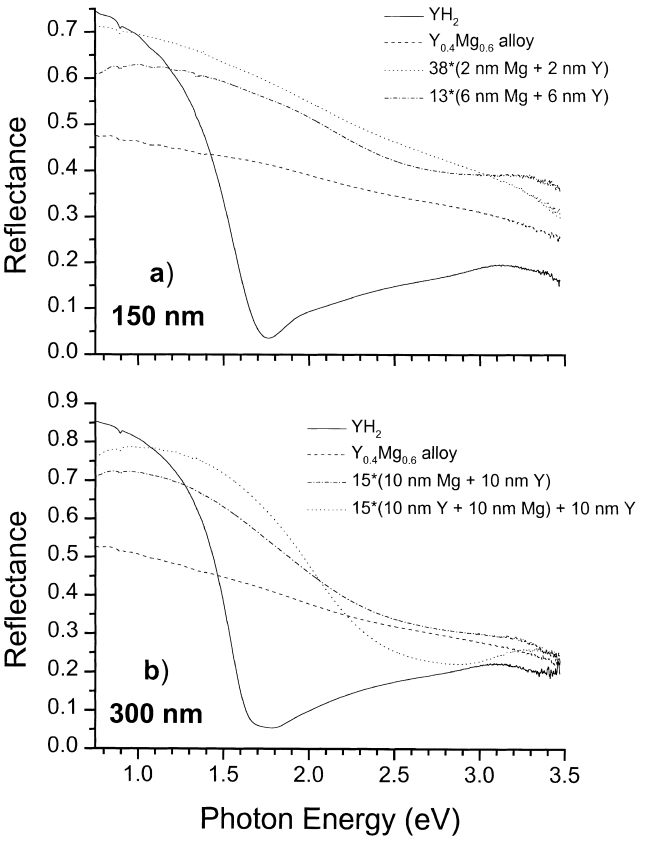

Fig. 2. Reflectance spectra after hydrogen desorption of the disordered $Y_{0.4}Mg_{0.6}H_{0.8}$ alloy, $Y_{0.4}Mg_{0.6}H_{0.8}$ multilayers, and YH_2 between 1700 and 350 nm. The films have a total thickness of (a) 150 nm, (b) 300 nm.

Summarizing, in the multilayered films the character of the two different materials, YH_x and MgH_x, can clearly be distinguished. The low-hydrogen phase is characterized by a shifted plasma energy of the YH_2-layers and a high reflectance of the Mg-layers. In the high-hydrogen phase the multilayers have a lower transmittance and become yellow again (for layer thicknesses >2 nm) because of the YH_3-layers.

3.2. Switching behaviour and thermodynamic properties

The switching behaviour of Y/Mg–H_x multilayers is studied in situ with high-angle XRD and electrochemical methods in combination with transmittance and resistivity measurements. A typical example of an X-ray/resistivity/transmittance experiment during hydrogen loading is shown in Fig. 3. In region I the resistivity drops slightly when hcp Y disappears and the better conducting fcc YH_2 phase appears. Therefore, the resistivity is lowest when the

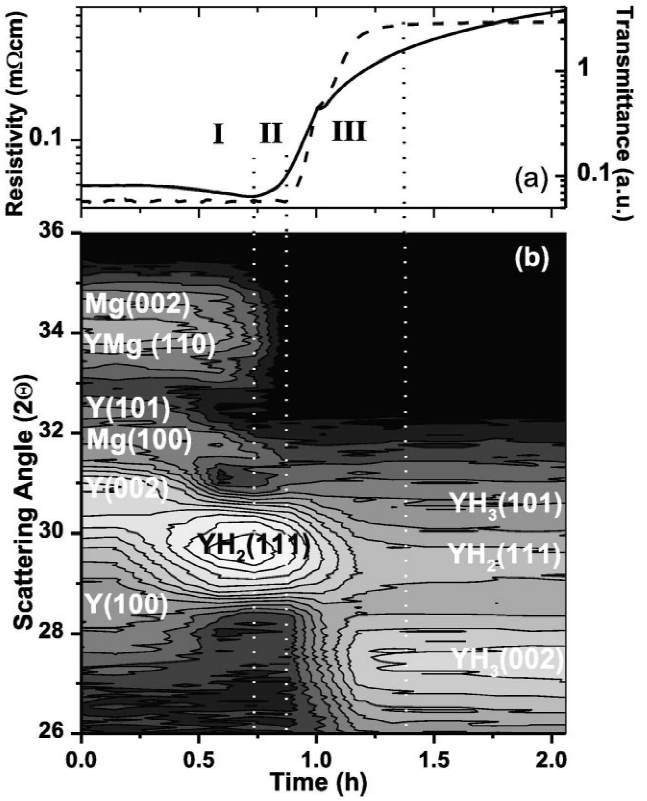

Fig. 3. Time evolution of (a) transmittance at 635 nm (1.96 eV) (dashed line) and resistivity (solid line); (b) Contour plot of the X-ray intensity as a function of time in a 13*(6 nm Mg +6 nm Y) multilayer capped by a 10 nm Pd layer. At $t=0.18$ h hydrogen gas at 20 mbar is introduced into the system. The grayscale corresponds to a logarithmic intensity scale.

intensity of the YH_2 peak is highest [2]. After that, in region II, the resistivity starts to rise again *before* an increase in transmittance is appearing. Together with this rise the YMg-intermetallic (with CsCl structure) and hcp Mg phases disappear. They are both gone at the onset of the transmittance (region III) when the main hcp YH_3 peak appears. Therefore, we conclude from the XRD measurements that the Mg starts to transform to MgH_2 before the YH_2 transforms to YH_3. Unfortunately, the rutile MgH_2 cannot be seen in XRD spectra because of its low scattering cross section compared to YH_x. We observe the same in the $Y_{0.4}Mg_{0.6}H_x$ alloys in agreement with the observations of Nagengast et al. [9].

To avoid effects related to the kinetics of hydrogenation we employ the Galvanostatic intermittent titration technique (GITT) to study the physical properties of electrochemically loaded Y/Mg–H_x multilayers (for more details see Ref. [12]). This technique enables us to construct pressure–composition isotherms for the Y/Mg–H_x multilayers as a function of the hydrogen concentration (see Fig. 4). The reversible region between the low-hydrogen phase where Mg coexists with YH_2, and the high hydrogen phase, where MgH_2 coexists with YH_3, is displayed.

In the pressure–composition isotherm of the 15*(10 nm Mg +10 nm Y) multilayer a plateau occurs before the onset of the transmittance. Such a plateau corresponds to a coexistence region between two phases. This indicates that either YH_2 or Mg is transforming into YH_3 or MgH_2, respectively. From the XRD measurements we concluded that Mg starts transforming before YH_2.

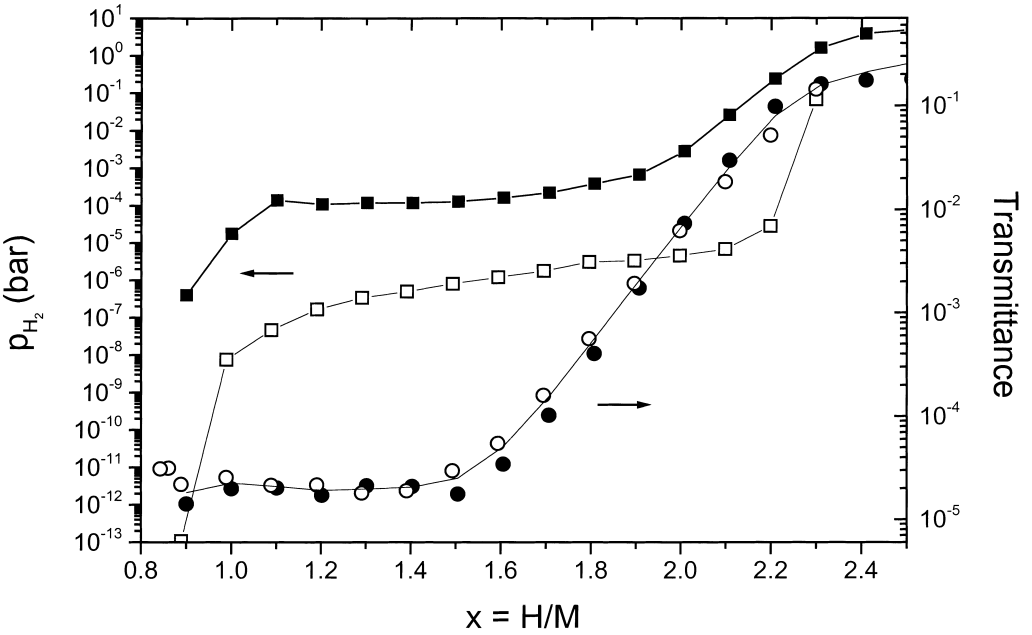

Fig. 4. Pressure–composition isotherm (squares) of a 15*(10 nm Mg+10 nm Y) ML capped with 10 nm Pd between the low-(YH_2 and Mg) and high-hydrogen phase (YH_3 and MgH_2) as a function of the hydrogen concentration per metal atom, $x=H/M$. Measurements are performed using GITT. The accuracy of x is ± 0.1. Also shown is the transmittance (circles) at 635 nm (1.96 eV). The filled symbols refer to hydrogen absorption and the open ones to desorption.

However, there is an overlap because the transmittance increases gradually (see Figs. 3 and 4) and the dihydride transmittance window of YH_2 (see Section 1) is not observed. In contrast, Nagengast et al. [9] concluded that in the alloys, Mg transforms totally to the transparent MgH_2 *before* the YH_2 becomes YH_3.

From the plateau pressures (in bar) in Fig. 4 we calculate the enthalpy of formation, ΔH_f, in J/mol H using the Van't Hoff relation [21]

$$\ln p_{H_2} = \frac{2\Delta H_f}{RT} + \frac{S^0_{H_2}}{R}, \quad (2)$$

where $S^0_{H_2} = 130.8$ J/K·mol H_2 is the standard molar entropy of hydrogen gas. In Table 2 the calculated ΔH_f are shown together with literature values.

The enthalpies of formation in the 10 nm ML are higher than the literature values for YH_3 formation except for the value found by Huiberts et al. [27]. They coincide, however, with the values found by Krozer et al. [24] for thin Mg films covered with a Pd cap layer for hydrogen absorption as well as for desorption. The enthalpies for the formation of MgH_2 obtained in GdMg and YMg alloys are, however, much lower and comparable to bulk values. This is related to a higher stress/strain state in the alloys than in the multilayers. Because of this Mg does not transform to the normal rutile MgH_2 but to orthorhombic MgH_2 in the alloys [9]. Moreover, the metallic Mg lattice is expanded compared to pure Mg films and therefore, the enthalpy of formation is more negative than in thin Mg-films and multilayers [9,21]. Because the stress/strain state in multilayers is lower compared to alloys the formation of MgH_2 can be as likely as the conversion of YH_2 to YH_3. Nevertheless, the multilayers switch optically faster than disordered alloys in agreement with the observation of Van der Sluis et al. [19].

A striking feature of the multilayers is that almost no hysteresis is observed in the transmittance in sharp contrast to pure YH_x [3], whereas the isotherms do show hysteresis (see Fig. 4). In Fig. 5 the transmittance of the 15*(10 nm Mg + 10 nm Y) ML is compared to that of a 300 nm YH_x-film. The suppression of the dihydride YH_2 transmittance window due to the presence of highly reflective Mg in the multilayers and alloys (see also Section 3.1) leads to a large contrast between the non-transparent (reflective) and transparent states of at least four orders of magnitude (see Fig. 5). Pure YH_x has a contrast of only two orders of magnitude in absorption and one in desorption [3] (see Fig. 5). The contrast in reflectance is, however, limited by the reflection of the Pd cap layer in the transparent state.

4. Conclusions

The optical behaviour of $Y/Mg–H_{2.4}$ multilayers with increasing individual layer thicknesses shows that their absorption edge is shifted in energy from the edge of the alloy $Y_{0.4}Mg_{0.6}H_{2.4}$ towards that observed in the pure YH_3 film. Thus, the transmittance and the absorption edge of the YMg-films are non-trivially dependent on the Mg distribution in the film. Moreover, the optical contrast of multilayers is much higher than for pure YH_x. The reflectance of the multilayers is superior to the alloys whereas the transmittance of the RE–Mg alloys is superior to the multilayers. From the in situ XRD and thermodynamic measurements combined with transmittance measurements we conclude that Mg and YH_2 transform almost at the same time to MgH_2 and YH_3, respectively, with a heat of formation of -30.9 kJ/mol H in absorption and -36.6 kJ/mol H in desorption. Strikingly, the multilayers do not exhibit disadvantageous hysteretic effects in the transmittance in sharp contrast with YH_x. This and their superior reflectance make multilayers especially attractive for devices.

Acknowledgements

The authors thank S.J. van der Molen for fruitful discussions. This work is part of the research program of the Stichting voor Fundamenteel Onderzoek der Materie

Table 2
Heat of formation, ΔH_f, in kJ/mol H in absorption (ab) at room temperature and desorption (des) of MgH_2 and YH_3. In the REMg alloys it is indicated whether the value corresponds to the formation of MgH_2 or REH_3

Sample	Reference	ΔH_f^{ab}	ΔH_f^{des}
Bulk Mg	[22]	−37.2	
	[23]	−38.3 (mean value)	−36.8
Thin films of Mg/Pd	[24]	−30.4±3.2	−35.6±2.1
Bulk Y	[25]	−41.8	
	[26]	−43.1	−42.2
Thin films of Y/Pd	[3]	$-37.4 < \Delta H < -32.7$	−44.8
	[27]	−30.0	
15*(10 nm Mg + 10 nm Y)/10 nm Pd	This work	−30.9	−36.6
200 nm $Gd_{0.38}Mg_{0.62}$/10 nm Pd	[28]	MgH_2: −41	
400 nm $Y_{0.5}Mg_{0.5}$/15 nm Pd	[9]	MgH_2: −42	
	[9]	YH_3: −31	

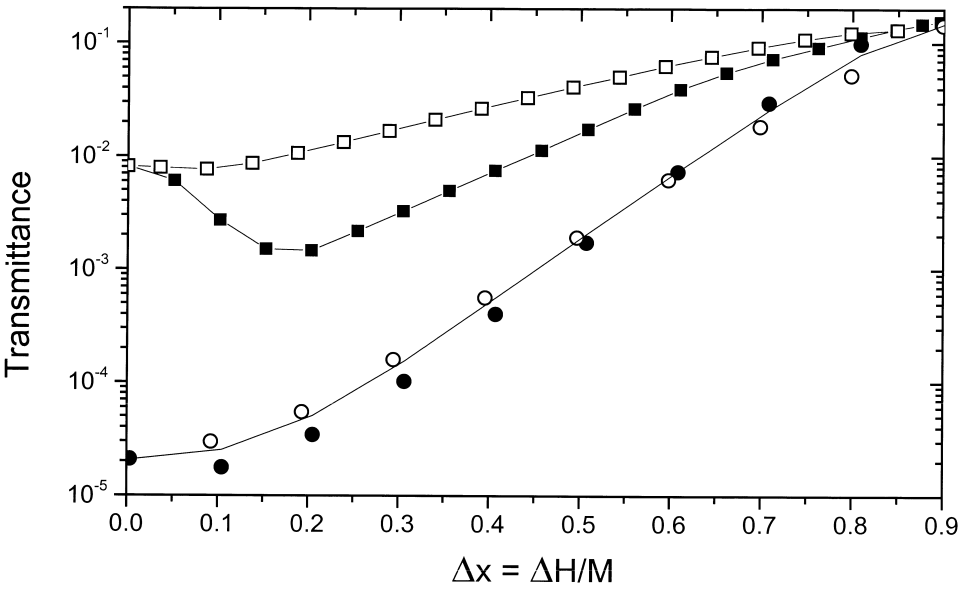

Fig. 5. Optical transmittance at 1.96 eV as a function of the relative concentration change per metal atom, ΔH/M, for a 300 nm Y film (squares) and a Y/Mg–H_x ML with 15*(10 nm Mg +10 nm Y), (circles) in hydrogen absorption (filled symbols) and desorption (open symbols). Measurements were performed using GITT. The resolution of the spectrometer is limited to 10^{-5}.

(FOM), financially supported by the Nederlandse Organisatie voor Wetenschappelijk Onderzoek (NWO), and of the TMR Research Network 'Metal-hydride films with switchable physical properties'.

References

[1] J.N. Huiberts, R. Griessen, J.H. Rector, R.J. Wijngaarden, J.P. Dekker, D.G. de Groot, N.J. Koeman, Yttrium and lanthanum hydride films with switchable optical properties, Nature 380 (1996) 231–234.

[2] M. Kremers, N.J. Koeman, R. Griessen, P.H.L. Notten, R. Tolboom, P.J. Kelly, P.A. Duine, Optical transmission spectroscopy of switchable yttrium hydride films, Phys. Rev. B 57 (8) (1998) 4943–4949.

[3] E.S. Kooij, A.T.M. van Gogh, D.G. Nagengast, N.J. Koeman, R. Griessen, Hysteresis and the single-phase metal–insulator transition in switchable YH_x, Phys. Rev. B 62 (15) (2000) 10088–10100.

[4] A.T.M. van Gogh, D.G. Nagengast, E.S. Kooij, N.J. Koeman, J.H. Rector, R. Griessen, C.F.J. Flipse, R.J.J.G.A.M. Smeets, Structural, electrical and optical properties of $La_{1-z}Y_zH_x$ switchable mirrors, Phys. Rev. B 63 (2001) 195105-1–195105-21.

[5] P. van der Sluis, M. Ouwerkerk, P.A. Duine, Optical switches based on magnesium lanthanide alloy hydrides, Appl. Phys. Lett. 70 (25) (1997) 3356–3358.

[6] M. Ouwerkerk, Electrochemically induced optical switching of $Sm_{0.3}Mg_{0.7}H_x$, Solid State Ionics 115 (1998) 431–437.

[7] K. von Rottkay, M. Rubin, P.A. Duine, Refractive index changes of Pd-coated magnesium lanthanide switchable mirrors upon hydrogen insertion, J. Appl. Phys. 85 (1) (1999) 408–413.

[8] K. von Rottkay, M. Rubin, F. Michalak, R. Armitage, T. Richardson, J. Slack, P.A. Duine, Effect of hydrogen insertion on the optical properties of Pd-coated magnesium lanthanides, Electrochim. Acta 44 (1999) 3093–3100.

[9] D.G. Nagengast, A.T.M. van Gogh, E.S. Kooij, B. Dam, R. Griessen, Contrast-enhancement of rare-earth switchable mirrors through microscopic shutter effect, Appl. Phys. Lett. 75 (14) (1999) 2050–2052.

[10] S.J. van der Molen, D.G. Nagengast, A.T.M. van Gogh, J. Kalkman, J.H. Rector, R. Griessen, Insulating fcc-$YH_{3-\delta}$ stabilized by MgH_2, accepted for publication in Phys. Rev. B.

[11] P.H.L. Notten, M. Kremers, R. Griessen, Optical switching of Y-hydride thin film electrodes, J. Electrochem. Soc. 143 (10) (1996) 3348–3353.

[12] E.S. Kooij, A.T.M. van Gogh, R. Griessen, In situ resistivity measurements and optical transmission and reflection spectroscopy of electrochemically loaded switchable YH_x films, J. Electrochem. Soc. 146 (1999) 2990–2994.

[13] R. Armitage, M. Rubin, T. Richardson, N. O'Brien, Y. Chen, Solid-state gadolinium–magnesium hydride optical switch, Appl. Phys. Lett. 75 (13) (1999) 1863–1865.

[14] L.J. van der Pauw, A method of measuring specific resistivity and Hall effect of discs of arbitrary shape, Philips Res. Rep. 13 (1) (1958) 1–9.

[15] A. Fischer, R. Fasel, J. Osterwalder, A. Krozer, L. Schlapbach, Mg on Pd(111): The formation of local order observed by photoelectron diffraction, Phys. Rev. Lett. 70 (10) (1993) 1493–1496.

[16] K. Yamamoto, K. Higuchi, H. Kajioka, H. Sumida, S. Orimo, H. Fujii, Optical transmission of magnesium hydride thin film with characteristic nanostructure, J. Alloys Comp. 330–332 (2002) 352–356.

[17] E.J. Johnson, Absorption near the fundamental edge, in: Optical Properties of III–V Compounds of Semiconductors and Semimetals, Vol. 3, Academic Press, New York, 1967, Chapter 6.

[18] J. Tauc, R. Grigorovici, A. Vancu, Optical properties and electronic structure of amorphous germanium, Phys. Status Solidi 15 (1966) 627–637.

[19] P. van der Sluis, Optical switches of gadolinium–magnesium multilayers, Appl. Phys. Lett. 73 (13) (1998) 1826–1828.

[20] J.H. Weaver, R. Rosei, D.T. Peterman, Electronic structure of metal hydrides. I. Optical studies of ScH_2, YH_2, and LuH_2, Phys. Rev. B19 (10) (1979) 4855–4866.

[21] R. Griessen, T. Riesterer, Heat of formation models, in: Topics in Applied Physics – Hydrogen in Intermetallic Compounds, Vol. 63, Springer-Verlag, Berlin, 1988, Chapter 6.

[22] W.M. Mueller, J.P. Blackledge, G.G. Libowitz (Eds.), Metal Hydrides, Academic Press, New York, 1968.

[23] B. Bogdanović, K. Bohmhammel, B. Christ, A. Reiser, K. Schlichte,

R. Vehlen, U. Wolf, Thermodynamic investigation of the magnesium–hydrogen system, J. Alloys Comp. 282 (1999) 84–92.
[24] A. Krozer, B. Kasemo, Hydrogen uptake by Pd-coated Mg: Absorption–decomposition isotherms and uptake kinetics, J. Less-Common Met. 160 (1990) 323–342.
[25] H.E. Flotow, D.W. Osborne, K. Otto, B.M. Abraham, YH_3 and YD_3: Heat capacities and thermodynamic functions from 15 to 350 K and infrared absorption spectra, J. Chem. Phys. 38 (11) (1963) 2620–2626.
[26] L.N. Yannopoulos, R.K. Edwards, P.G. Wahlbeck, The thermodynamics of the yttrium–hydrogen system, J. Phys. Chem. 69 (8) (1965) 2510–2514.
[27] J.N. Huiberts, J.H. Rector, R.J. Wijngaarden, S. Jetten, D. de Groot, B. Dam, N.J. Koeman, R. Griessen, B. Hjörvarsson, S. Olafsson, Y.S. Cho, Synthesis of yttriumtrihydride films for ex-situ measurements, J. Alloys Comp. 239 (1996) 158–171.
[28] M. Di Vece, J.J. Kelly, to be published.